Guidance on the use of meteorological time series constructed to match the KNMI'23 climate scenarios

version 1.0

Henk van den Brink, Cees de Valk

KNMI, De Bilt, October 9, 2023

Contents

Part I. Guidance

1 Introduction

In the previously issued KNMI climate scenarios Klein Tank et al. (2014), time-series of weather observations were transformed to time-series representative of scenarios for future climates, using climate change signals (such as differences in monthly percentiles of temperature) extracted from climate model projections. These data were used to produce various data products linked to the scenarios, and the time-series themselves were made available for the assessment of the impacts of the climate scenarios. In addition, external users were enabled to perform this transformation on their own time-series, either off-line (by a stand-alone program) or online through the KNMI Climate Explorer.

For the KNMI '23 climate scenarios van Dorland et al. (2023), a different approach has been adopted: in addition to time-series of transformed observations, also bias-corrected climate model projections are provided; see van Dorland et al. (2023). The bias-corrected climate model projections are available for all 12 km $\times$ 12 km grid cells of the RACMO regional climate model. They have also been used to compute the climate change signal in the scenario tables; see van Dorland et al. (2023), Section 2.1.11.

Bias-corrected climate model projections are suitable for a range of applications, but not for all. Therefore, in addition, observed time-series transformed to match the climate change signals corresponding to the four scenarios considered are provided for the sites with daily precipitation measurements, with data of other variables taken from the nearest automated weather station.

The two datasets (bias-corrected model projections and transformed time-series of observations) each have their strengths and weaknesses. For each application, these need to be considered carefully before deciding which dataset is to be used.

This document provides guidance for this decision, as well as a little background on the methods used to provide the data and how they differ from the methods used previously for transforming observed time-series (see KNMI (2015))). Further explanation of the bias-correction of model projections and the transformation of observed time-series can be found in the Appendix of this document, which reproduces relevant sections from van Dorland et al. (2023). General guidance on the use of the KNMI '23 climate scenarios can be found in Chapter 11 of van Dorland et al. (2023).

2 Brief overview of the methods

2.1 Basic principles

The method selected for bias-correction of RACMO data as well as for transformation of time-series of observations is the Quantile Delta Mapping (QDM) (Cannon et al. (2015)).

For a given probability p, a quantile $Q(p)$ is the value exceeded with probability $1-p$. We assume that Q is a continuous function which increases on $(0,1)$. So if F

is the cumulative distribution function, then $F(Q(p)) = p$ and $Q(F(x)) = x$.

The QDM method corrects primarily quantiles. Applied for bias correction of the quantile $Q_f(p)$ for a future climate scenario, the quantile delta mapping (QDM) method assumes that quantiles of simulations change in the same way as quantiles in the real world, as time goes by. "In the same way" can mean different things. For temperature, surface pressure (mslp) and humidity, we assume that differences between quantiles for the future climate and the reference ("historical") climate are the same in the simulations as in the real world, so for each probability p,

$$\hat{Q}_f(p) = Q_o(p) + Q_f(p) - Q_r(p), \tag{1}$$

with

$Q_o(p)$ the quantile of the observations over the reference period,

$Q_r(p)$ the quantile of the simulations for the reference climate,

$Q_f(p)$ the quantile of the simulations for the future climate,

$\hat{Q}_f(p)$ the bias-corrected quantile for the future climate.

Another way to describe this is that QDM preserves the "climate signal" consisting of the differences between the quantiles corresponding to the future and the historical climate.

The correction $\hat{x}_f(t)$ of a projection $x_f(t)$ at day t is obtained by applying (1) to the probability of not exceeding the simulated future value for day t, $F_f(x_f(t))$:

$$\hat{x}_f(t) = \hat{Q}_f\big(F_f(x_f(t))\big), \tag{2}$$

with F_f the cumulative distribution function for the similated future climate.

The method is illustrated in Figure A3 (top). The black line shows the cumulative distribution function (CDF) of (in this illustration) the observed temperature, which is the reference. The blue line is the CDF of the historical RACMO temperature, which shows a positive bias that depends on the quantile. The blue arrows (the "deltas") indicate how much the temperature quantiles for the probabilities of 0.05, 0.25, 0.50, 0.75 and 0.95 need to be adjusted in order to agree with the reference quantiles.

The red curve in Figure A3 (top) represents the CDF of the uncorrected RACMO data for the future run (solid red line). It maps each uncorrected RACMO temperature for the future to a probability. Then the blue arrow (delta) for this probability is added to the temperature to yield the bias-corrected temperature. The bias-corrected future temperatures therefore have the CDF indicated by the dashed red curve in Figure A3 (top).

The time-series transformation of a measured temperature record $x_o(t)$ is theoretically almost the same: we also compute (1), but then

$$\hat{x}_f(t) = \hat{Q}_f\big(F_o(x_o(t))\big) \tag{3}$$

with F_o the cumulative distribution function of the observations; compare also Figure A3 (bottom) to Figure A3 (top).

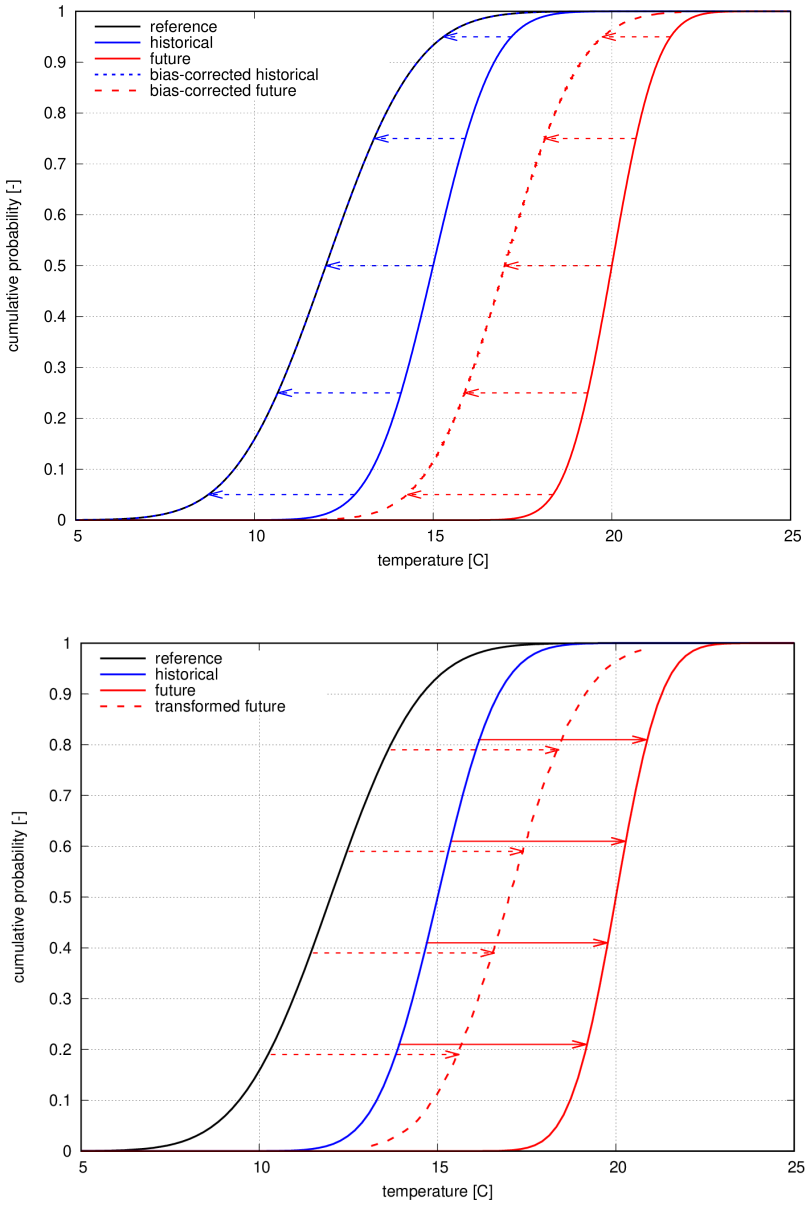

Fig. 1: Graphical explanation of the Quantile Delta Mapping method for bias-correction (top) and for time-series transformation (bottom) of temperature.

In theory, therefore, the only difference between bias correction by QDM and time-series transformation by QDM is in the temporal ordering of the values: this ordering is different for $F_o(x_o(t))$ (derived from the observed values) than for $F_f(x_f(t))$ (derived from the model projection for the future climate).

This similarity between bias-correction and time-series transformation using QDM has been one of the main reasons for choosing QDM. Other reasons are that its computation is relatively stable (important for the tails), and that it performs relatively well in tests on climate model simulations and measurements for past 30-year periods.

In practice, there are other differences between bias-correction and time-series transformation, since we need to approximate and smooth the quantiles in (1) (see Section 2.2). Furthermore, the lengths (in days) of the observed and simulated time-series are not the same (van Dorland et al. (2023)), so we cannot even compute an exact empirical QDM from the data; interpolation or smoothing is always needed. Depending on the application, the effects of these differences determine whether bias-correction or time-series transformation is more useful; see Section 3.

For precipitation, surface wind speed and global radiation, not the differences, but the **ratios** of future and reference values are assumed to be the same in the simulations and in the real world, so instead of (1), we assume

$$\hat{Q_f}(p) = Q_o(p)Q_f(p)/Q_r(p). \tag{4}$$

Other than this, the procedure is the same as for temperature etc.

2.2 Implementation

The Quantile Delta Mapping is approximated by computing only the quantiles and the changes in quantiles (differences or ratios) for the following probabilities: 0, 0.001, 0.01, 0.05, 0.1, 0.15, 0.2, 0.25, 0.3, 0.35, 0.4, 0.45, 0.5, 0.55, 0.6, 0.65, 0.7, 0.75, 0.8, 0.85, 0.9, 0.95, 0.99, 0.999, 0.9999. For other probabilities, the changes in quantiles are obtained by linear interpolation. The following comments are made:

- the 0.99, 0.999 and 0.9999 quantiles are not directly calculated, but extrapolated from the 0.90 and 0.95 quantiles. For precipitation, we use the exponential distribution for this extrapolation, for the wind, the Weibull distribution, and for the temperature, the Gaussian distribution is applied. In this way, stochastic uncertainty in the extreme quantiles is reduced. However, despite this, one cannot expect that the mapping of extreme values will be accurate. For the other variables (humidity, mslp, radiation), no extrapolation is applied (as here the extremes are not very relevant).

- The gridded observational data for precipitation is discretized in steps of 0.05 mm, and the rain gauge observations are discretized in steps of 0.1 mm. This distorts the bias correction or time-series transformation for low precipitation amounts, and consequently the number of dry days (often defined as days with less than 0.1 mm). The largest quantiles that indicate no precipitation are therefore adjusted to small precipitation amounts (i.e. drizzle). This is done by extrapolating from the lowest wet quantiles, as long as the

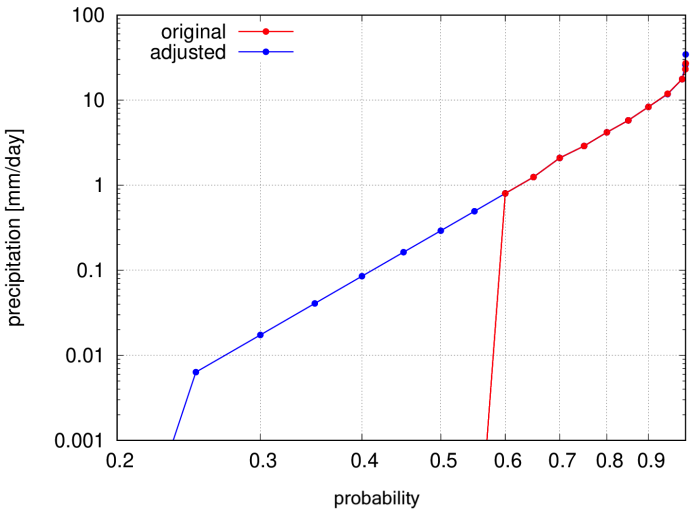

Fig. 2: Illustration of the wetting of the quantiles that indicate no precipitation. Both axes are logarithmic.

adjusted precipitation is larger than 0.005 mm. These quantiles are adjusted by linear extrapolation on a logarithmic scale. The adjustment is graphically explained in Figure A4. In this example, the original (red) CDF indicates 'dry' for quantiles of 0.55 and below. The quantiles of 0.6 and 0.65 are used for the extrapolation down to the threshold of 0.005 mm.

Bias correction was applied separately to each of the 12 km × 12 km grid cells of the RACMO model, using gridded observations (see Table 2.5 of van Dorland et al. (2023)). Time series transformation is performed for every site of 24-h precipitation measurements (of the order of 300 sites scattered over the Netherlands), using data from the nearest weather station for other variables than precipitation, and using RACMO model output from the nearest grid cell over land.

Both bias-correction and time-series transformation are computed separately for each month of the year, in order to capture seasonality in the bias or in the climate change signal.

Note that both bias-correction and time-series transformation only adjust quantiles (or equivalently, distribution functions); persistence is not corrected. This works out differently for the two methods: bias correction cannot correct errors in simulated persistence (but can preserve simulated changes in persistence); time-series transformation cannot preserve simulated changes in persistence. The same caveat applies to other aspects such as inter-variable dependence, and spatial dependence.

Further information is found in the Appendix.

2.3 Differences with the methods applied in KNMI'14

KNMI'14 Klein Tank et al. (2014), offered only transformed time-series of observations of temperature, precipitation and global radiation (and of derived quantities ptential evapotranspiration, precipitation deficit and relative change in relative humidity); see KNMI (2015). No bias-corrected model projections were provided, and

no data of relative humidity, global radiation and wind speed.

Differences in methodology are briefly summarized below.

For temperature, the methods are very similar (both QDM), except that in KNMI'23, many more probability levels considered. The impact of this is limited, however, because temperature bias consists mostly of a constant shift.

For precipitation, KNMI'14 applied a rather complex time-series transformation: wet-days (with more than 0.05 mm of precipitation) were separated from dry days, and the relative change in the conditional wet-day mean and 99% quantile of precipitation from the simulations were preserved in the transformation. Also, the relative change in the fraction of wet days from the simulations was preserved, and "wetting" or "drying" of days was performed in a sophisticated manner which preserved the temporal clustering of wet and dry days in the observations as much as possible. However, this method cannot preserve simulated changes in persistence other than due to changes in the distribution of precipitation (see Section 2.5.1 of van Dorland et al. (2023)). In KNMI'23, wet and dry days are no longer separated; we simply extrapolate the quantiles to low probabilities ad apply a straightforward QDM; see Section 2.2. The idea behind this is that if persistence is important (e.g. for precipitation deficit, or river discharge), one can now use the bias-corrected RACMO simulations instead of the transformed time-series of observations; these preserve the simulated changes in persistence. Note howeveer that these are valid on the spatial scale of a RACMO grid cell (12 km), and not for a point (rain gauge).

For radiation, the simple linear correction applied in KNMI'14 is replaced by the standard discrete QDM method.

3 Relative strengths and weaknesses of time-series transformation and bias-correction

There is no perfect method for constructing time-series representative of scenarios for future climates. Therefore, KNMI'23 offers both bias-corrected model simulations and transformed time-series of observations. Each has potential drawbacks, summarized in Table 1. Note that it is not relevant how many potential issues are listed for a method; its suitability for a particular application can only be judged by examining each issue to assess how serious it is and how much it impacts the application.

Furthermore, there may be practical reasons for preferring a dataset, such as consistency with previous impact assessments.

	Possible issues	bias-corrected simulations	transformed TS of observations
1	the time-series are too short to draw firm conclusions about rare and extreme events	✓	✓
2	randomness distorts the simulated change in the extreme quantiles	✓	
6	changes in persistence, spatial or inter-variable dependence cannot be accounted for		✓
5	spatial or inter-variable dependence or persistence may be biased due to model limitations	✓	
4	spatial or inter-variable dependence may be distorted due to combining data from different sites		✓
7	bias correction may distort the climate change signal from the model	✓	
3	a TS transformation or bias-correction may be distorted due to a climate change signal within the time-series from which it is computed	✓	✓

Tab. 1: List of potential issues with time series representative of scenarios for future climates, with an indication of which method is potentially affected most by the issue.

1. Users should should be aware that the time-series as provided cover relatively short periods, so regardless of the method, it may not be warranted to draw firm conclusions about extreme events from these time-series. A model may produce a larger dataset (e.g. an ensemble) for a given climate. If this is the case, then bias-correction may produce more data for the user; on the other hand, a time-series transformation may be more accurately calibrated based on the model data. Observations cover 30 years, so the bias correction or time-series transformation for a given month is based on approximately $30 \times 30 = 900$ data points in total. This means that the 99th percentile is already quite inaccurate: even though it is determined by extrapolation from the 90th and 95th percentiles, it is also affected by extrapolation error. Therefore, we advice against using these bias corrections or time-series transformations straightforwardly in an extreme value analysis without carefully addressing the possible errors.

2. Simulated time-series for the present climate and for scenarios for the future climate are statistically independent. Therefore, just by chance, a simulation for the present climate may contain a very extreme precipitation sum, while the simulation for a future climate may not have such rare values. These inevitable random differences can strongly distort changes in the statistics of extremes, in particular for variables such as precipitation with heavy-tailed dis-

tributions. Bias-correction does not improve this. Therefore, bias-corrected climate model simulations may not be suitable for studying changes in extremes. Transformed time-series of observations are not affected in the same way by this specific issue, but random differences between simulated time-series for the present climate and for scenarios for the future climate may still affect the transformation estimated from these data, so caution is also warranted in this case (see also item 1.).

3. Transformed TS of observations retain the persistence, spatial and inter-variable dependence of the observations (note that we apply a separate transformation for each variable). Therefore, a simulated change in these dependencies over time will not be expressed in the transformed time-series data: persistence, spatial and inter-variable dependence in the resulting time-series are essentially the same for the climate scenarios as in the reference climate.

4. Spatial smoothness, persistence and/or inter-variable dependence in simulations may be biased due to limitations on model resolution and representation of physical processes (e.g. the soil water balance, or the relationship between warming and extreme rainfall). This affects primarily bias-corrected model projections. Biased spatial smoothness in simulations may also affect a time-series transformation, if this transformation depends strongly on spatial scale; however, we do not have concrete evidence of this for daily values.

5. Transformed TS of observations are provided at all sites of 24-hour precipitation measurements. For temperature, global radiation and relative humidity, data are taken from the nearest weather station, which can be at considerable distance. This may affect the inter-variable dependence, but also the spatial dependence. On the positive side, temperature, global radiation and relative humidity vary less in space than precipitation, which reduces the impact. For the same reasons, we advice caution and restraint with spatial interpolation or spatial averaging of the daily values of transformed time-series. We would advice to consider instead interpolating or averaging of climate indices (statistics) computed from the individual time series.

6. Bias correction using the QDM method has the property that simulated absolute or relative changes in quantiles over time are preserved in the bias-corrected time-series. This in itself minimizes distortion of the simulated climate change signal by the bias correction. However, distortion is still possible, for example if the wrong choice is made between preserving absolute or relative change. Our choices are consistent with the literature and informed by physical knowledge about inter-relationships between variables, such as the approximately linear dependence of the logarithm of (extreme) precipitation on absolute temperature according to (or proportional to) the Clausius-Clapeyron relation. However, as no assumption is perfect, some bias will still be present.

7. Quantiles used in the transformation (1) may be distorted due to a climate change signal within the time-series from which they were computed. In particular, this may increase the spread in values. For bias-correction, this may

be a problem in particular if the trends in the historical simulation and the observations are not the same. For a time-series transformation, it may cause bias if the trends in the current and future climate are very different.

4 How to obtain the data

The time-series data representative of scenarios for future climates can be obtained from `https://klimaatscenarios-data.knmi.nl/`. This archive contains time-series of bias-corrected model projections as well as transformed time-series of observations (see Section 3).

This website will also contain any updates to the present document.

References

Bakker, A. and J. Bessembinder (2015). Time series transformation tool: Description of the program to generate time series consistent with the knmi'60 climate scenarios, report tr-349. Technical report.

Buiteveld, H. and M. Eberle (2005). Hydrological modelling in the river rhine basin: Daily hbv model for the rhine basin. Technical Report dl. 3.

Cannon, A. J., S. R. Sobie, and T. Q. Murdock (2015). Bias correction of gcm precipitation by quantile mapping: How well do methods preserve changes in quantiles and extremes? *Journal of Climate 28*(17), 6938–6959.

Casanueva, A., S. Herrera, M. Iturbide, S. Lange, M. Jury, A. Dosio, D. Maraun, and J. M. Gutiérrez (2020). Testing bias adjustment methods for regional climate change applications under observational uncertainty and resolution mismatch. *Atmospheric Science Letters 21*(7), e978.

Cornes, R. C., G. van der Schrier, E. J. M. van den Besselaar, and P. D. Jones (2018). An ensemble version of the e-obs temperature and precipitation data sets. *Journal of Geophysical Research: Atmospheres 123*(17), 9391–9409.

Feigenwinter, I., S. Kotlarski, A. Casanueva, C. Schwierz, and M. Liniger (2018). Exploring quantile mapping as a tool to produce user-tailored climate scenarios for switzerland. Technical report, MeteoSchweiz.

François, B., M. Vrac, A. J. Cannon, Y. Robin, and D. Allard (2020). Multivariate bias corrections of climate simulations: which benefits for which losses? *Earth System Dynamics 11*(2), 537–562.

Klein Tank, A., J. Beersma, J. Bessembinder, B. Van den Hurk, and G. Lenderink (2014). Knmi 14: Klimaatscenario's voor nederland. *KNMI publicatie*.

KNMI (2015). KNMI'14 Toelichting transformatie tijdreeksen. `https://cdn.knmi.nl/knmi/asc/knmi14/transformatieprogramma/Toelichting_TP.pdf`. [Online; version 6-10-2015].

Rauthe, M., H. Steiner, U. Riediger, A. Mazurkiewicz, and A. Gratzki (2013). A central european precipitation climatology – part i: Generation and validation of a high-resolution gridded daily data set (hyras). *Meteorologische Zeitschrift 22*, 235–256.

van Dorland, R., J. Beersma, J. Bessembinder, N. Bloemendaal, H. van den Brink, M. B. Blanes, S. Drijfhout, R. Haarsma, I. Keizer, F. Krikken, D. L. Bars, G. Lenderink, E. van Meijgaard, J. F. Meirink, T. Reerink, F. Selten, C. Severijns, P. Siegmund, A. Sterl, B. Overbeek, H. de Vries, B. W. Schreur, and K. van der Wiel (2023). Knmi national climate scenarios 2023 for the netherlands. Technical Report WR23-02, Royal Netherlands Meteorological Institute.

van Verseveld, W. J., A. H. Weerts, M. Visser, J. Buitink, R. O. Imhoff, H. Boisgontier, L. Bouaziz, D. Eilander, M. Hegnauer, C. ten Velden, and B. Russell (2022). Wflow-sbm v0.6.1 - a spatially distributed hydrologic model: from global data to local applications. *Geoscientific Model Development Discussions 2022*, 1–52.

Whan, K., J. Zscheischler, A. I. Jordan, and J. F. Ziegel (2021). Novel multivariate quantile mapping methods for ensemble post-processing of medium-range forecasts. *Weather and Climate Extremes 32*, 100310.

Part II. Appendix: Detailed documentation and data-analysis

The following is a reproduction of Sections 2.1.10 and 2.5.1 in van Dorland et al. (2023). Further context can be found in the same report.

A1 Bias correction of resampling output

A1.1 Introduction

There are several reasons why the RACMO climatology differs from the observed climatology

- due to natural variability, the climatology of RACMO will always differ from the observed climatology. This effect will be most pronounced for the extremes.
- due to difference in resolution: the observations are local, whereas RACMO values are averaged over 12 km $\times$ 12 km.
- some meteorological processes (e.g. convection) are poorly resolved by RACMO, which may lead to underestimation of extreme (summer) precipitation.
- the roughness map of RACMO may differ from reality (e.g. by seasonal changes due to more or less leafs on the trees).
- the orography of RACMO may - especially in the Alps - be too low, again due to averaging over the grid size. This may influence variables like temperature (too high in RACMO) and precipitation (too low in RACMO).
- The climatological forcing from EC-Earth3bis may be wrong, which leads to biases in the climatology of RACMO.
- the resampling is optimised to resemble the *signal* from the CMIP6 models; a part of this signal may be achieved by distorting the control climate.

For these reasons, bias in the RACMO data is corrected. We applied bias correction to each variable, month and location separately, using the Quantile Delta Mapping (QDM) from Cannon et al. (2015) (see also Chapter 5 in Feigenwinter et al. (2018) for an extensive description):

- For each probability in (0,1), the difference or ratio (the "delta") of the quantiles of the observations ("truth") and the RACMO output is assumed to be the same in the present and the future climate. This determines the quantiles of the bias-corrected RACMO output for the future climate for all these probabilities.
- Then the uncorrected RACMO output for the future climate is adjusted to match these quantiles.

A1.2 Methodology for bias correction

Quantile Delta Mapping The method of Quantile Delta Mapping (Cannon et al. (2015)) is illustrated in Figure A3. The black line shows the empirical cumulative distribution function (ECDF) of (in this illustration) the observed temperature, which is the reference. The blue line is the ECDF of the historical RACMO temperature, which shows a positive bias that depends on the quantile. The blue arrows (the "deltas") indicate how much the temperature quantiles for the probabilities of 0.05, 0.25, 0.50, 0.75 and 0.95 need to be adjusted in order to agree with the reference quantiles.

The red curve in Figure A3 represents the ECDF of the uncorrected RACMO data for the future run (solid red line). It maps each uncorrected RACMO temperature for the future to a probability. Then the blue arrow (delta) for this probability is added to the temperature to yield the bias-corrected temperature. The bias-corrected future temperatures therefore have the ECDF indicated by the dashed red curve in Figure A3.

For temperature, mslp and humidity, the *differences* of the quantiles of the observations and of the RACMO output for the historical period (the arrows in Figure A3) are preserved in the future climate for every probability, as described above. However, for precipitation, surface wind and radiation, we preserve the *ratios* (except for zero values; see details below). This can be reduced to the previous case by taking logarithms.

Comparing the bias-corrected model output to the observations (our reference), the climate signal from the RACMO simulations of temperature, mslp and humidity is preserved in the following sense (see Figure A3): for every probability, the horizontal differences between the dashed red and solid black lines are identical to the corresponding horizontal differences between the solid red and blue lines. In other words, the *absolute* changes in quantiles computed by RACMO constitute the preserved climate signal. Similarly, for precipitation, surface wind and radiation, the *relative* changes in the quantiles computed by RACMO are now the preserved climate signal.

The Quantile Delta Mapping is approximated by computing only the quantiles and the changes in quantiles (differences or ratios) for the following probabilities: 0, 0.001, 0.01, 0.05, 0.1, 0.15, 0.2, 0.25, 0.3, 0.35, 0.4, 0.45, 0.5, 0.55, 0.6, 0.65, 0.7, 0.75, 0.8, 0.85, 0.9, 0.95, 0.99, 0.999, 0.9999. For other probabilities, the changes in quantiles are obtained by linear interpolation. The following comments are made:

- the 0.99, 0.999 and 0.9999 quantiles are not directly calculated, but extrapolated from the 0.90 and 0.95 quantiles. For precipitation, we use the exponential distribution for this extrapolation, for the wind, the Weibull distribution, and for the temperature, the Gaussian distribution is applied. In this way, stochastic uncertainty in the extreme quantiles is reduced. However, despite this, one cannot expect that the mapping of extreme values will be accurate. For the other variables (humidity, mslp, radiation), no extrapolation is applied (as here the extremes are not very relevant).

- the gridded observational data for precipitation is discretized in steps of 0.05 mm, which distorts the bias correction for low precipitation amounts, and conse-

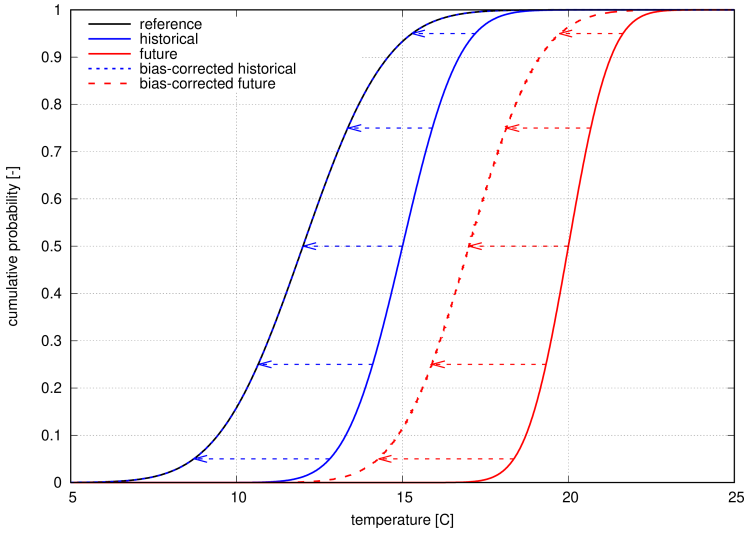

Fig. A3: Explanation of the Quantile Delta Mapping method.

quently the number of dry days (often defined as days with less than 0.1 mm). The largest quantiles that indicate no precipitation are therefore adjusted to small precipitation amounts (i.e. drizzle). This is done by extrapolating from the lowest wet quantiles, as long as the adjusted precipitation is larger than 0.005 mm. These quantiles are adjusted by linear extrapolation on a logarithmic scale. The adjustment is graphically explained in Figure A4. In this example, the original (red) ECDF indicates 'dry' for quantiles of 0.55 and below. The quantiles of 0.6 and 0.65 are used for the extrapolation down to the threshold of 0.005 mm.

Besides the Quantile Delta Mapping, a number of other methods have been proposed for bias-correction: other simple univariate methods (e.g., ordinary Quantile Mapping or simple linear transformations, e.g. Cannon et al. (2015), Casanueva et al. (2020)) but also complex multivariate bias-correction methods; see e.g. François et al. (2020), Whan et al. (2021).

For the present study, it was decided to select a simple univariate method and to test it on indices derived from multiple variables such as multi-day averages, computed river discharge, precipitation deficit and fire weather index, in order to find out if the selected method is good enough for the climate scenarios.

From the simple methods, the Quantile Delta Mapping was selected because it is relatively robust (except possibly in the extreme ranges, like all other methods), has produced good results in other studies (e.g. Cannon et al. (2015)) and shows relatively good performance in tests based on historical weather data over two different periods. Moreover, Quantile Delta Mapping can also be used for transformation of time-series of observations to a future climate (see Section A2.2), and the results of bias-correction and time-series transformation using Quantile Delta Mapping are highly compatible.

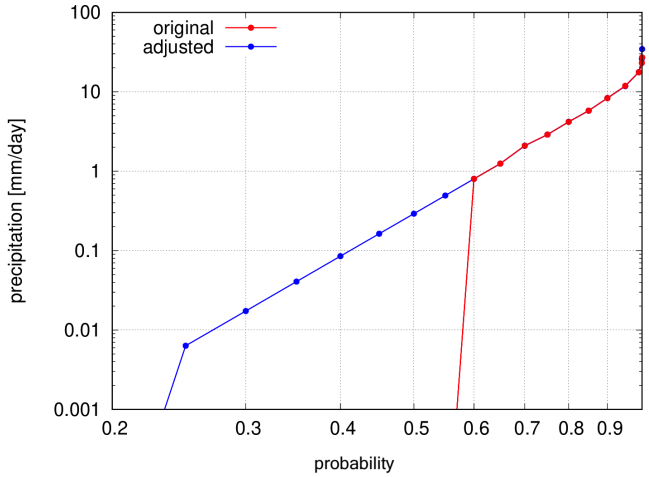

Fig. A4: Illustration of the wetting of the quantiles that indicate no precipitation. Both axes are logarithmic.

A1.3 Description of the gridded observations

Table 2 lists the variables that are bias-corrected, as well as the datasets of gridded observations used for this purpose.

variable:	dataset:
minimum temperature	EOBSv26e
maximum temperature	EOBSv26e
mean temperature	EOBSv26e
wind speed	EOBSv26e
precipitation	HYRAS3.0-PR (+EOBSv26e)
radiation	SARAH-3

Tab. 2: variables that are bias-corrected, and the gridded dataset used.

EOBSv26e The data set covers the period back to 1950 and provides gridded fields at a spacing of 0.1deg × 0.1deg in regular latitude/longitude coordinates. The EOBS dataset is described in Cornes et al. (2018).

HYRAS3.0 The HYRAS3.0 dataset represents daily high-resolution (5 km × 5 km) grids of mean, minimum, and maximum temperature and relative humidity for Germany and its catchment areas, from 1951 to 2015. In addition to temperature and relative humidity, HYRAS-2015 also comprises a precipitation dataset (HYRAS-PR). This is an extension of the HYRAS-2006 version, presented in Rauthe et al. (2013).

The HYRAS3.0-PR dataset is preferred over the EOBSv26e dataset because of its higher spatial resolution, which is of importance especially in the Alps. In order

to extend this dataset to the 1991-2020 period, quantiles were derived from the 1986-2015 period for both HYRAS3.0-PR and EOBSv26e and applied to the 2016-2020 period of EOBSv26e. These bias-corrected data were concatenated to the 1991-2015 HYRAS3.0-PR data. For the areas outside the HYRAS3.0-PR domain, EOBSv26e was used.

We acknowledge the DWD for the use of the HYRAS dataset.

SARAH SARAH-3 was produced by the Satellite Application Facility on Climate Monitoring (CM SAF) from Meteosat geostationary satellite observations. It spans the years 1983 until present. The data record is not yet publicly available. It was kindly provided by Jörg Trentmann (Deutscher Wetterdienst).

The quantiles of the observational datasets are calculated on the original grids, and then regridded to the RACMO grid. In this way the influence of the regridding is minimized, as the spatial fields of the quantiles are much smoother than the fields of individual time steps (especially of precipitation).

The EOBS and HYRAS datasets only cover land. The missing values of the quantiles over sea are filled with the nearest land points. This implies that we assume that the climate signal over sea is similar to the signal in the coastal area. It may be clear that this assumption fails far from the coast, especially for e.g. temperature.

A1.4 Results

Illustration Figure A5 shows, for an arbitrary grid point in The Netherlands, the biases in the RACMO data (for the 2100Hn control resample[1]) with respect to the observations for January, April, July and October. The high ratios in winter for precipitation indicate that RACMO has considerable amount of drizzle, which is absent in summer. For extreme daily precipitation, the bias in RACMO is relatively small: the ratios tend to 1. The bias in temperature depends both on the season and on the quantile. In this example, the bias is small in July, except for the extremes, which are 1K too warm. The cold days in January are too cold in RACMO. Also for minimum and maximum temperature the biases are mostly within 1K. The deviation in radiation can be up to 20% in winter; however, here the values are small and of minor importance compared to summer values. The relative humidity values differ up to 5%-point in July.

Here we show how some relevant variables compare to the climatology of the gridded observations before and after bias correction.

annual cycle The annual cycle of the precipitation, temperature and PET are shown in Figure A6. In all cases, the bias is reduced, especially for the precipitation (which shows in the unbiased situations too high precipitation amounts in the winter and too low amounts in the summer.

[1] 2100Hn stands for wet ('nat') variant of the high scenario (i.e. SSP5-8.5) in 2100. See Table 3.3 for a more detailed description of the KNMI'23 climate scenarios names.

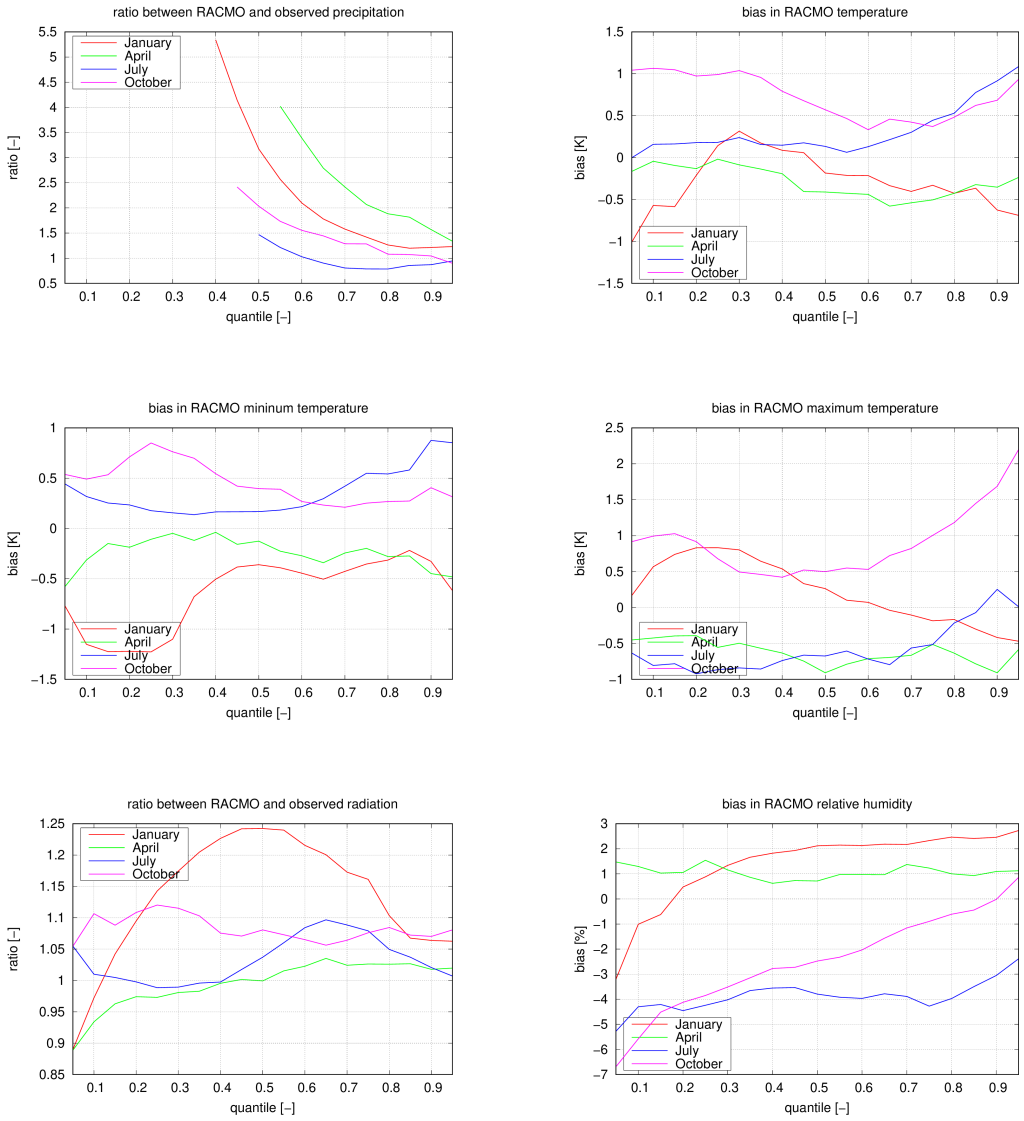

Fig. A5: Comparison of the quantiles in the observations and RACMO for an arbitrary grid point in The Netherlands. Shown are the lines for January, April, July and October for precipitation (a), temperature (b), minimum temperature (c) and maximum temperature (d), radiation (e) and relative humidity (f).

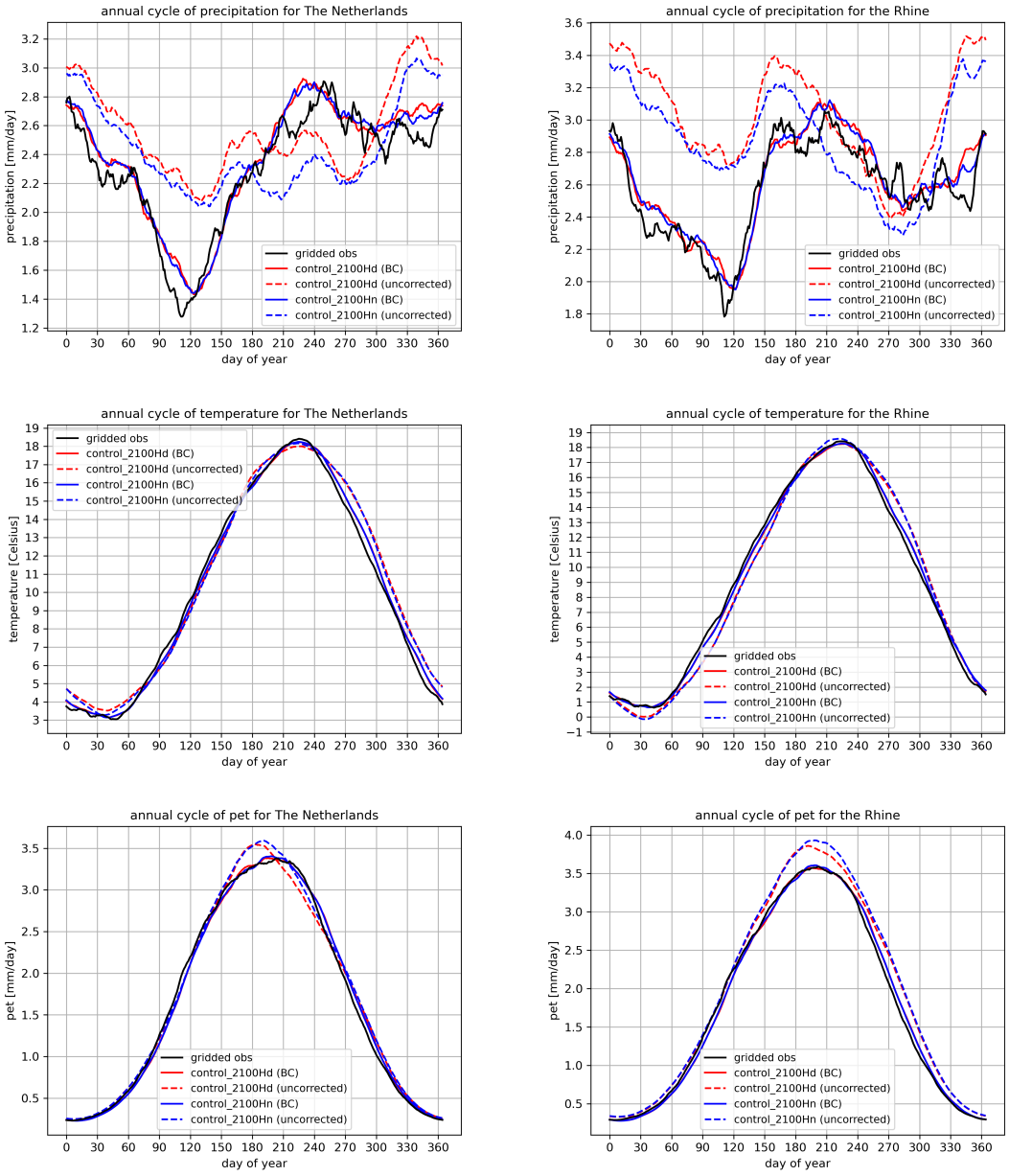

Fig. A6: Annual cycle of the precipitation, temperature and Potential Evapotranspiration (PET) for The Netherlands (left) and the Rhine (right). The dashed lines indicate the unbiased values for Hd (red) and Hn (blue), the solid lines are the bias-corrected lines.

Figure A7 shows, for the temperature in July, how well the 5%, 50% and 99.9% quantiles of the gridded observations compare to the quantiles that are calculated after bias-correction (ideally they should be equal). The left column shows in colors the gridded observations (EOBSv26e), and in contours the bias-corrected RACMO results. The right column shows the bias in K. The figure shows that the biases after correction are very small (and are partly due to the effect of regridding, which is clearly visible in the Alps). Even for the 99.9% the biases are mostly small, and randomly distributed.

Figure A8 shows the 95, 99 and 99.9% quantiles of the precipitation in July (we choose higher quantiles than for temperature, as the lower quantiles indicate no precipitation). The right column shows the ratio between RACMO and EOBSv26e. The figure shows that the biases after correction are small (and are partly due to the effect of regridding). Even for the 99.9% the biases are fairly small, and randomly distributed.

Extremes

Precipitation extremes Figure A9 shows the Gumbel plots of the 1-day and 10-day precipitation amounts averaged over The Netherlands, the Vecht and the Rhine, resp. The dashed lines are the unbiased values, the solid lines the bias-corrected values. The black lines show the observational data. The plots for The Netherlands indicates that the biascorrection improves the once-a-year value, but seems to worsen the values for more extreme amounts. Although the effect is less pronounced for the 10-day values, it is still present. It is remarkable that the bias correction works well for the Vecht - although this river basin is smaller than The Netherlands. And for the Rhine, the bias correction seems to have no effect on the 1-day extremes; however is considerably improves the 10-day extremes.

We conclude that it is very hard to correct extremes with return periods larger than once a year. This is mainly due to the large statistical uncertainty that is present (mainly in the short observational set). Nevertheless, the bias correction performs well for the Vecht and The Rhine basins (also for the Meuse, not shown), and improves the Gumbel plots for the accumulated precipitation over multiple days (which is important for river discharges).

Temperature maxima Figure A10 shows the Gumbel plots of the 1-day and 10-day averaged temperatures over The Netherlands, the Vecht and the Rhine, resp. The dashed lines are the unbiased values, the solid lines the bias-corrected values. The black lines show the observational data. The biases in the extreme temperatures are small, and well corrected.

Temperature minima Figure A11 shows the Gumbel plots of the 1-day and 10-day averaged minimum temperatures over The Netherlands, the Vecht and the Rhine, resp. The dashed lines are the unbiased values, the solid lines the bias-corrected values. The black lines show the observational data. The biases in the low temperatures are small, and the effect of the bias correction is small.

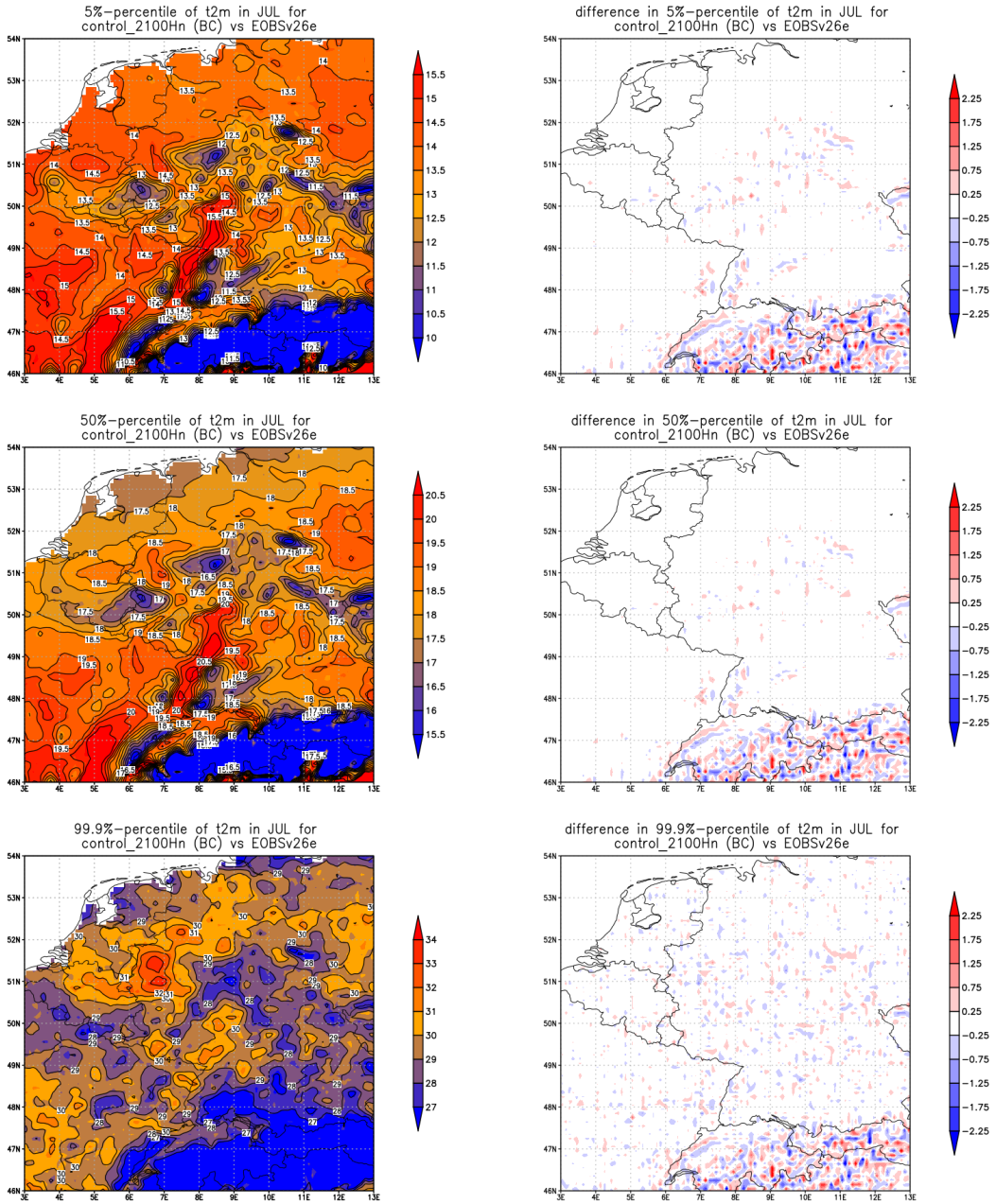

Fig. A7: Quantiles of the temperature in July for the gridded observations (EOBSv26e, shaded) and RACMO (contours), and the difference between RACMO and EOBSv26e (right).

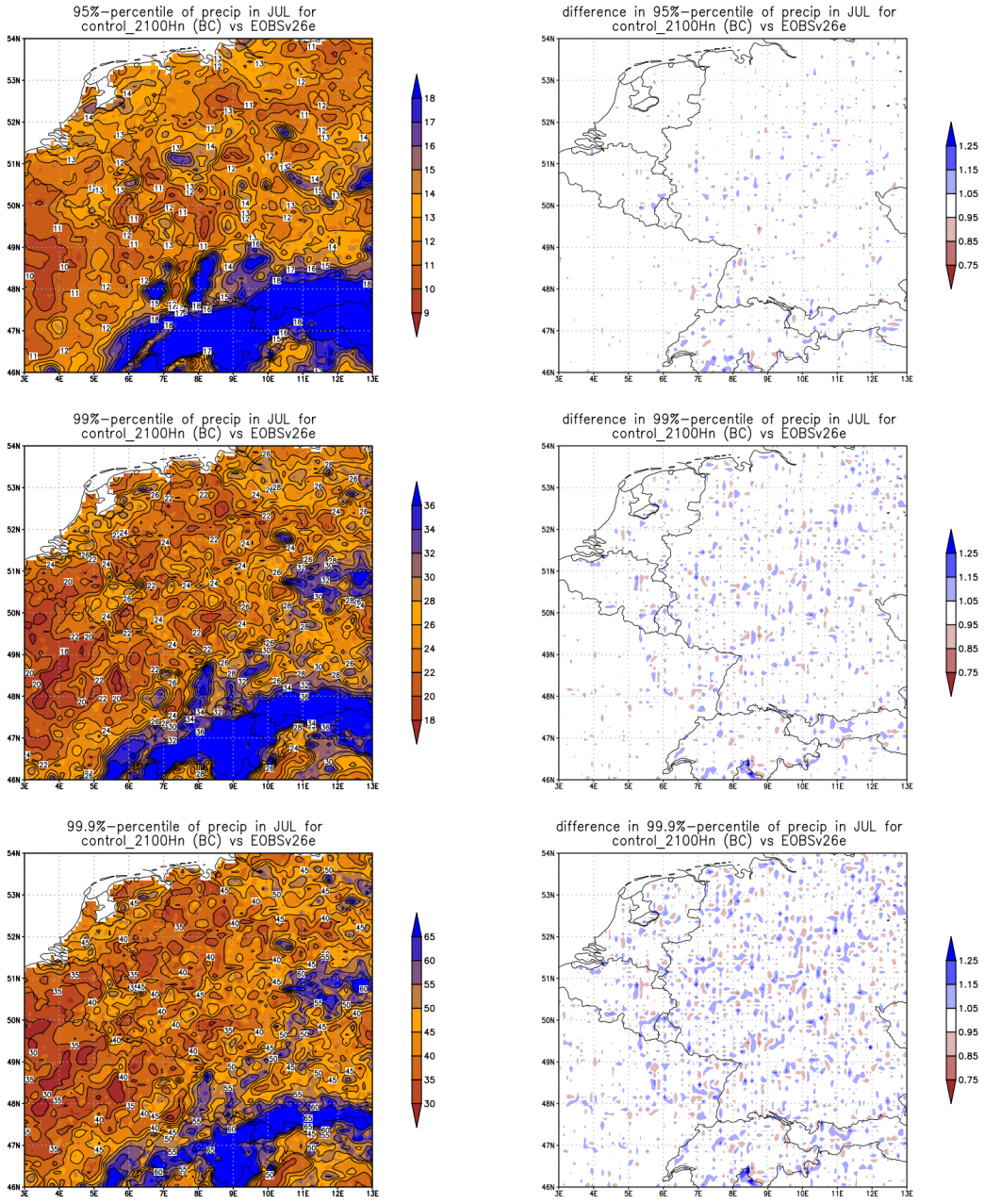

Fig. A8: Quantiles of the precipitation in July for the gridded observations (EOBSv26e, shaded) and RACMO (contours), and the ratio between RACMO and EOBSv26e (right).

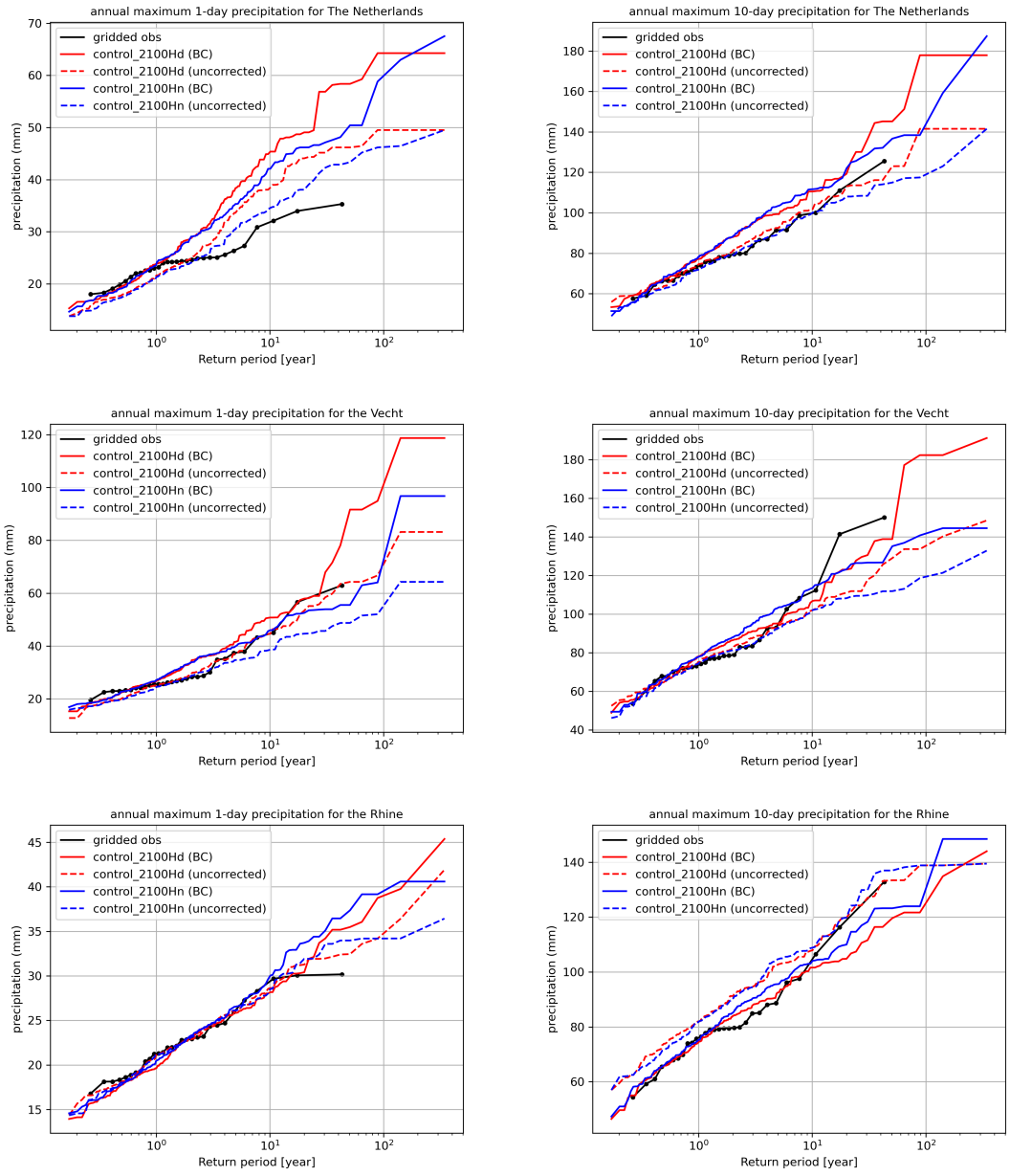

Fig. A9: Gumbel plots of the 1-day (left) and 10-day (right) precipitation for The Netherlands (upper), The Vecht (middle) and the Rhine (bottom). The dashed lines indicate the unbiased values for Hd (red) and Hn (blue), the solid lines are the bias-corrected lines.

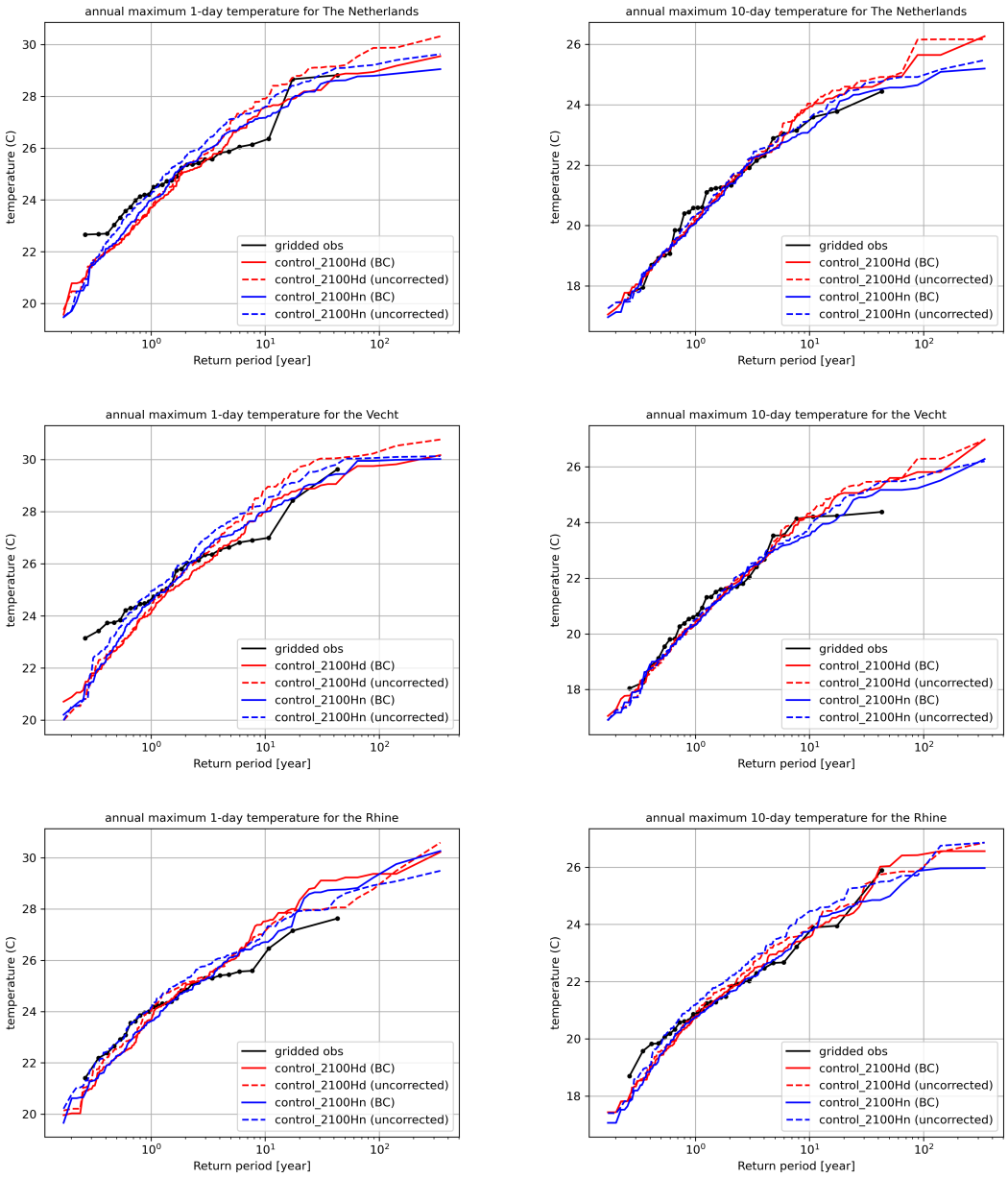

Fig. A10: Gumbel plots of the 1-day (left) and 10-day (right) temperature for The Netherlands (upper), The Vecht (middle) and the Rhine (bottom). The dashed lines indicate the unbiased values for 2100Hd (red) and 2100Hn (blue), the solid lines are the bias-corrected lines.

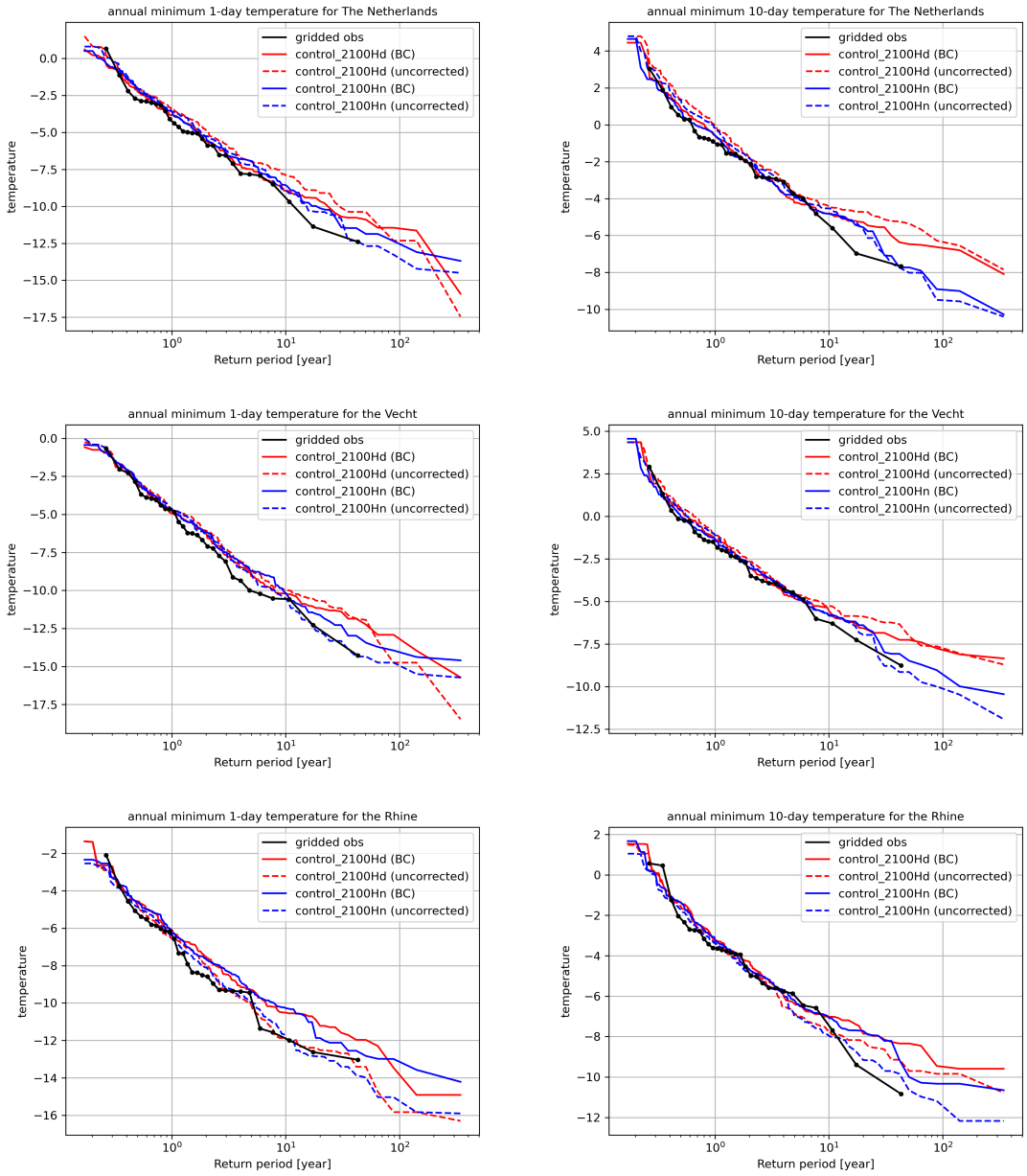

Fig. A11: Gumbel plots of the 1-day (left) and 10-day (right) minimum temperature for The Netherlands (upper), The Vecht (middle) and the Rhine (bottom). The dashed lines indicate the unbiased values for 2100Hd (red) and 2100Hn (blue), the solid lines are the bias-corrected lines.

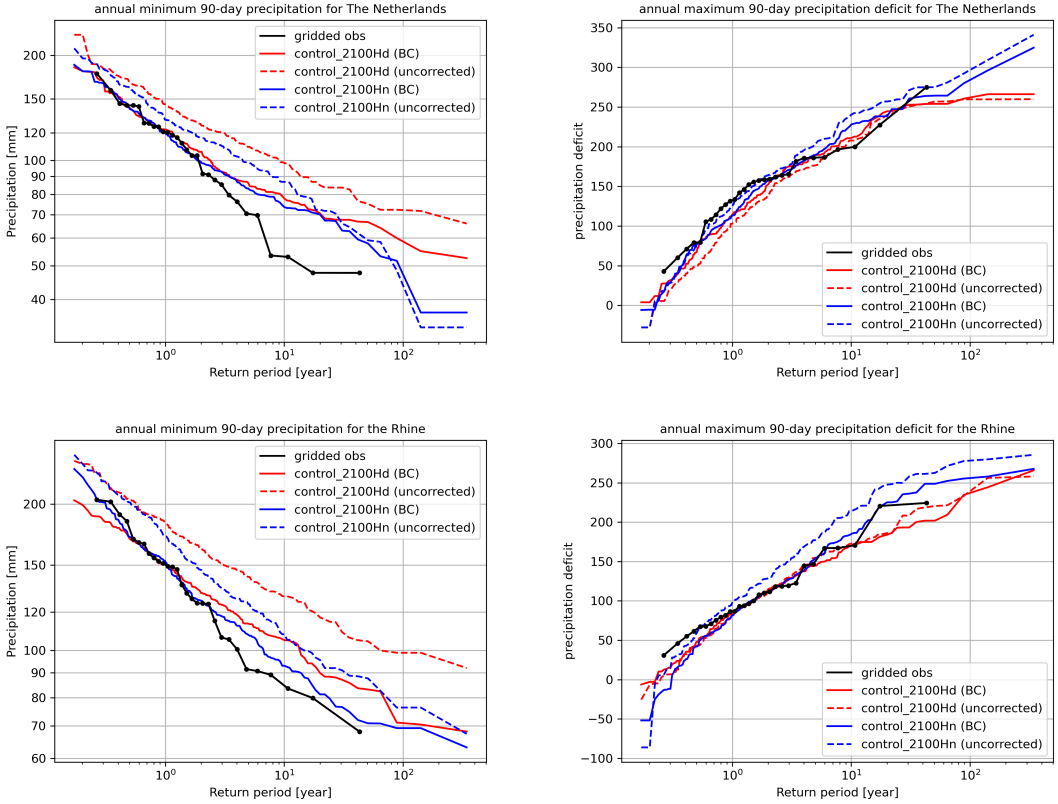

Fig. A12: Gumbel plots of the 90-day minimum precipitation (left) and precipitation deficit (right) for The Netherlands (upper) and the Rhine (bottom). The dashed lines indicate the unbiased values for 2100Hd (red) and 2100Hn (blue), the solid lines are the bias-corrected lines.

precipitation deficit Figure A12 shows the Gumbel plots of the minima of the cumulative precipitation over 90 days over The Netherlands and The Rhine basin. The right column shows the minimum values of the 90-day accumulated precipitation deficit (i.e., the cumulative amount of precipitation minus potential Evapotranspiration (pet)). The figure shows that the bias correction doesn't fully correct the overestimation of the most extreme precipitation minima (especially for The Netherlands), but that the precipitation deficit performs very well.

Figure A13 shows the temporal evolution through the year of the precipitation deficit for the grid point $(6\text{deg}E, 52\text{deg}N)$ for the uncorrected (left) and the biased scenarios. It shows that the bias is removed from the precipitation deficit for all three percentiles, for all three scenarios: after bias-correction they become indistinguishable in climatological sense. This indicates that RACMO represents realistic correlations both in time as well between the variables precipitation, radiation and temperature (which all influence the precipitation deficit).

River discharges In cooperation with Deltares, several bias-corrected 240-year runs each are used to calculate the discharges at Lobith (Rhine) and Borgharen (Meuse). This is done with the HBV model (Buiteveld and Eberle, 2005), as well with the (more advanced) model Wflow (van Verseveld et al., 2022). The Gumbel plots are shown in Figure A14. All Gumbel lines are similar (except the most extreme

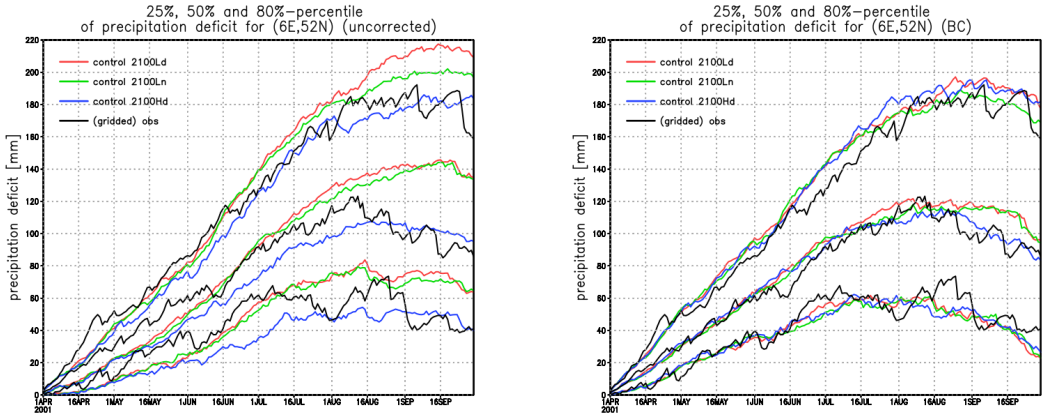

Fig. A13: Precipitation deficit without (left) and with (right) bias correction for the 25%, 50% and 80% percentiles for the gridded observations (black), and three control scenario's.

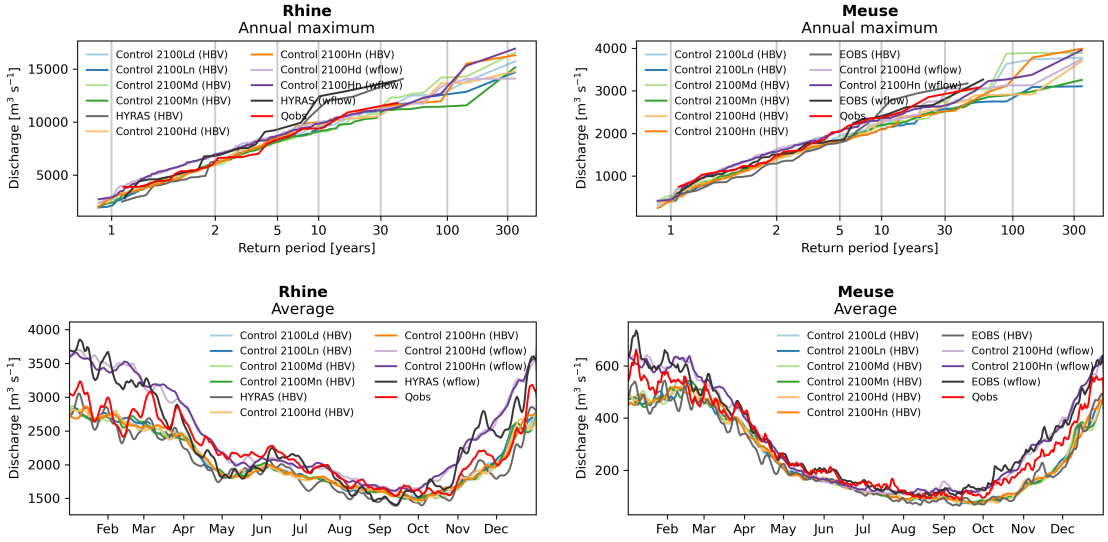

Fig. A14: Gumbel plots (top) of the extreme discharges in the Rhine (left) and the Meuse (left), and for the annual cycle (bottom).

events, due to statistical uncertainty). This is an extra confirmation that the bias-corrected meteorological variables have realistic correlations in time and space.

A2 Time series transformation

A2.1 Method

As an alternative to bias correction, a time-series of observations can be be transformed to obtain what these data would look like in future climate. This transformation can be designed to preserve a selected climate signal derived from the RACMO runs for the historical and the future climate. It was applied earlier to produce the KNMI'14 scenarios; see e.g. Bakker and Bessembinder (2015).

Bias correction of climate model simulations and time-series transformation (TT) each have their strengths and weaknesses, depending on purpose and specific circumstances:

- A time-series transformation starts from data with realistic dependencies in time and between different variables (e.g. the dependence between precipitation and humidity, or the distribution of the lengths of intervals without rain). Applying separate transformations for different variables preserves these dependencies, which may be an advantage if they are not well represented in the model output. However, this may be a drawback if the dependencies are realistic in the simulations, in particular if they change over time: such changes cannot be represented by time-series transformation.

- Another factor is the simplicity of the mapping(s) involved: for example, if the climate signal is simple (e.g. a uniform increase in temperature) but the bias has a complicated form, time-series transformation may have the practical advantage that it is easier to estimate from data. But the opposite may also be encountered: the bias may be simple and the climate-change signal may be complicated (e.g. changes may be different in the normal range of values and in the tail range).

- Furthermore, bias-corrected model data are available at all model grid points, whereas transformed time-series are only available at measurement sites. Therefore, bias-corrected model data may be more useful if spatial averages over specific regions are required

- Bias-corrected model data for a grid point are representative for a surrounding area, depending on the effective resolution of the model (in part determined by the processes resolved in the model). A transformed time-series represents only the site of the measurement.

- Another difference is that observational time-series for a given location are naturally limited in volume (typically to a 30-year period), whereas a model may produce a much larger dataset (e.g. an ensemble) for a given climate. If this is the case, then bias-correction may produce more data for the user; on the other hand, a time-series transformation may be more accurately calibrated from the model data.

- It is emphasised that the uncertainty in the extreme quantiles has the same impact on time-series transformation as it has on bias correction.

Results of time-series transformation and specific issues with the transformation for particular variables are discussed below section A2.2.

For the transformation of a time-series of observations, the Quantile Delta Mapping can also be used, just as for bias-correction of RACMO output: in the calculation, the roles of the observations and of the RACMO-output for the future climate are switched.

This is illustrated in Figure A15. The solid arrows show the climate signal from RACMO for a few quantiles. This signal is added (dashed arrows) to the quantiles of the observations (black line), which results in the the dashed cumulative distribution of the transformed time-series of observations.

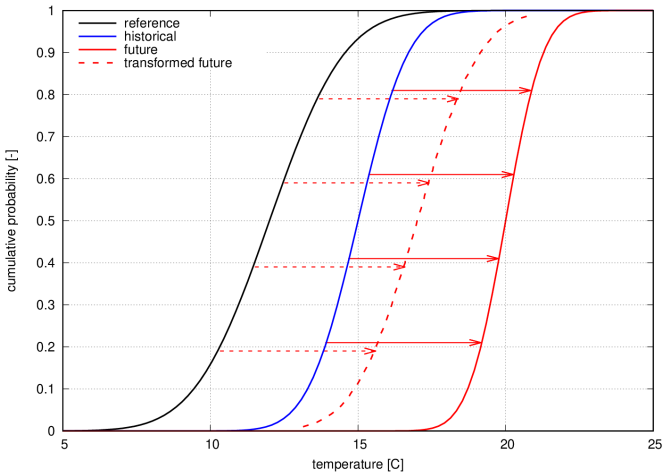

Fig. A15: Explanation of timeseries transformation method. The solid arrow show the climate signal in the (unbiased) RACMO data, the dashed arrows have similar lengths but are applied to the observed (black) distribution. The dashed distribution is identical to the dashed line in Figure A3.

Note that this dashed distribution is identical to the dashed line in Figure A3. This shows that using Quantile Delta Mapping for transforming a time-series of observations results in a time-series having (at least approximately) the same quantiles as when used to bias-correct the model output for the future climate. However, the temporal ordering of the ranks of the values will be different.

A2.2 Results of time-series transformation

In the figures below the climate signal in TT is compared with the signal as obtained from the RACMO resamples. Transformation of observed time series is only applied for The Netherlands, so in the figures only results for The Netherlands are shown. For the observations, the stations with daily precipitation measurements are used, supplemented with other meteorological parameters from the nearest station. Climate signals are only shown if the observed period (1991-2020) contains at least 20 years of data.

precipitation Figures A16 and A17 compare the signal in the transformed observed timeseries with the signal that comes directly from the RACMO runs. It shows that TT is able to reproduce the signal well, although small differences exist. Note the change from a drying trend in the 95%-percentile to a wetting trend in the 99%-percentile.

temperature The change in the 5%-percentile of the minimum temperature, the 50%-percentile average temperature and 95%-percentile maximum temperature in July are shown in Figure A18 for the 2100Hd scenario. Also here, TT reproduces the climate signal from RACMO well. Note the spatial difference in the warming:

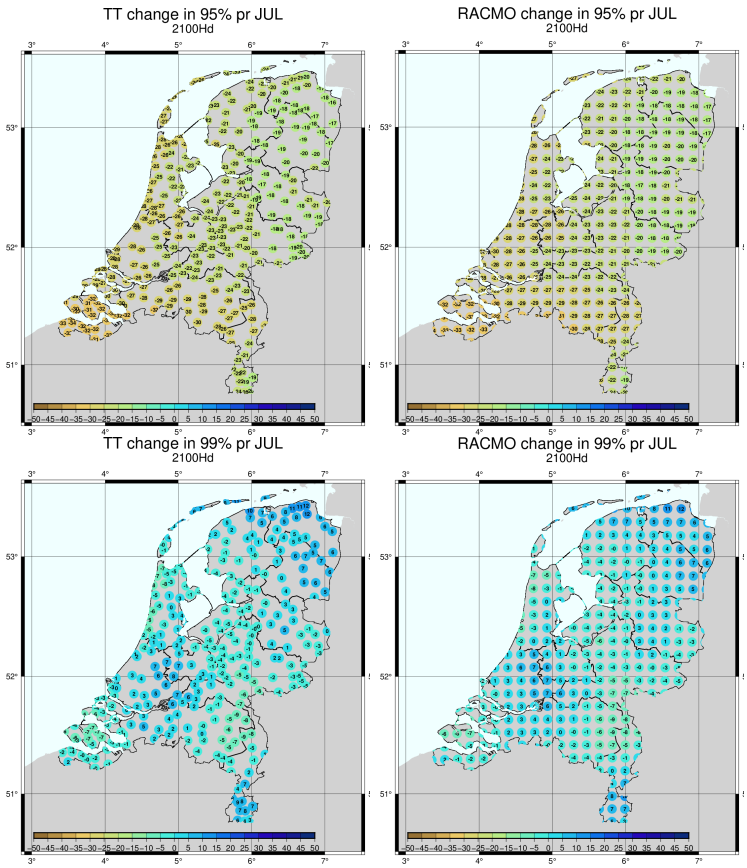

Fig. A16: Change in the 95% (upper) and 99% (lower) percentiles of the precipitation in July for timeseries transformation (left) and RACMO (right) for the 2100Hd scenario.

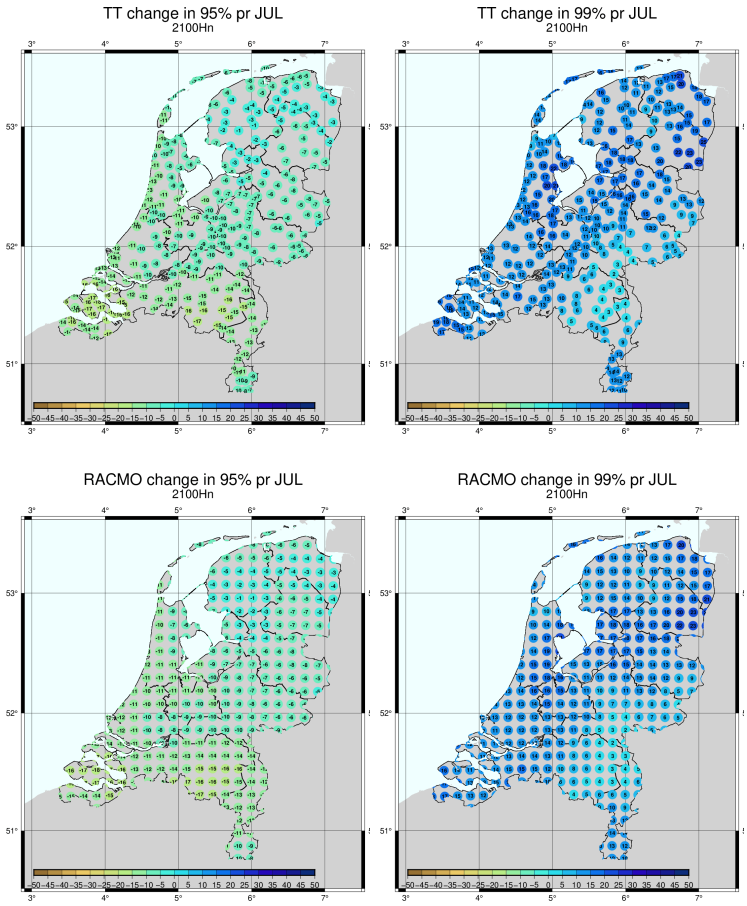

Fig. A17: Change in the 95% (left) and 99% (right) percentiles of the precipitation in July for timeseries transformation (upper) and RACMO (lower) for the 2100Hn scenario.

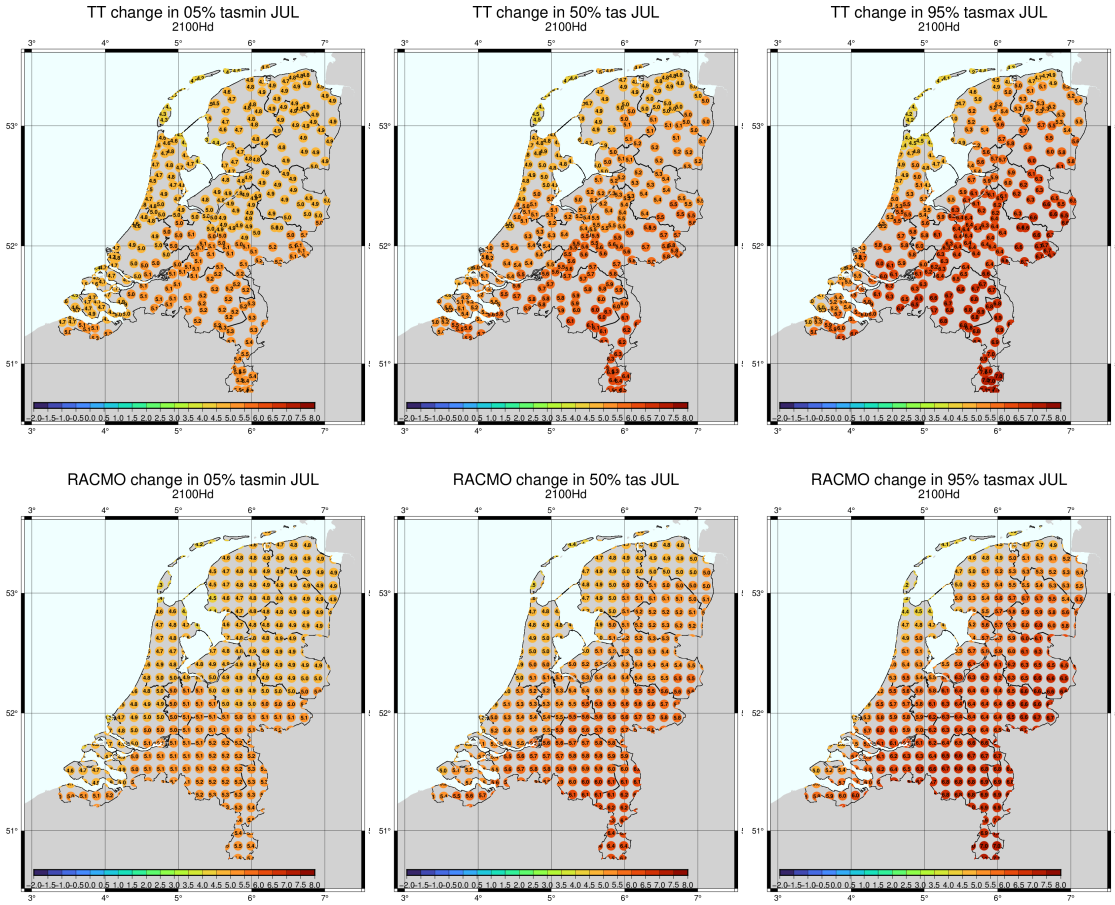

Fig. A18: Change in the 5%-percentile of the minimum temperature (left), the 50%-percentile average temperature (middle) and 95%-percentile maximum temperature (right) in July for timeseries transformation (upper) and RACMO (lower) for the 2100Hd scenario.

less along the coast and most in Limburg. Note also that the minimum temperature increases less than the average temperature, and the maximum temperature increases more than the average.

number of dry days Figure A19 shows the change in the number of dry days (defined as the number of days with less than 1mm of precipitation) according to TT and to BC. Also here the agreement is good.

duration of dry days Figure A20 shows the change in the number of consecutive dry days (defined as the number of days with less than 1mm of precipitation per day) according to TT and to BC. Here TT underestimates the change in the increase of consecutive dry day with approximately 50%. This indicates that the change in persistence is not fully captured by TT.

number of tropical days Figure A21 shows the number of tropical days (i.e., the maximum temperature exceeds 30°C) for the observations (left upper) and for BC (left lower). Also shown are the situations according to 2100Hn (middle column) and 2100Hd (right column). The number of tropical days for TT agrees well with the BC results.

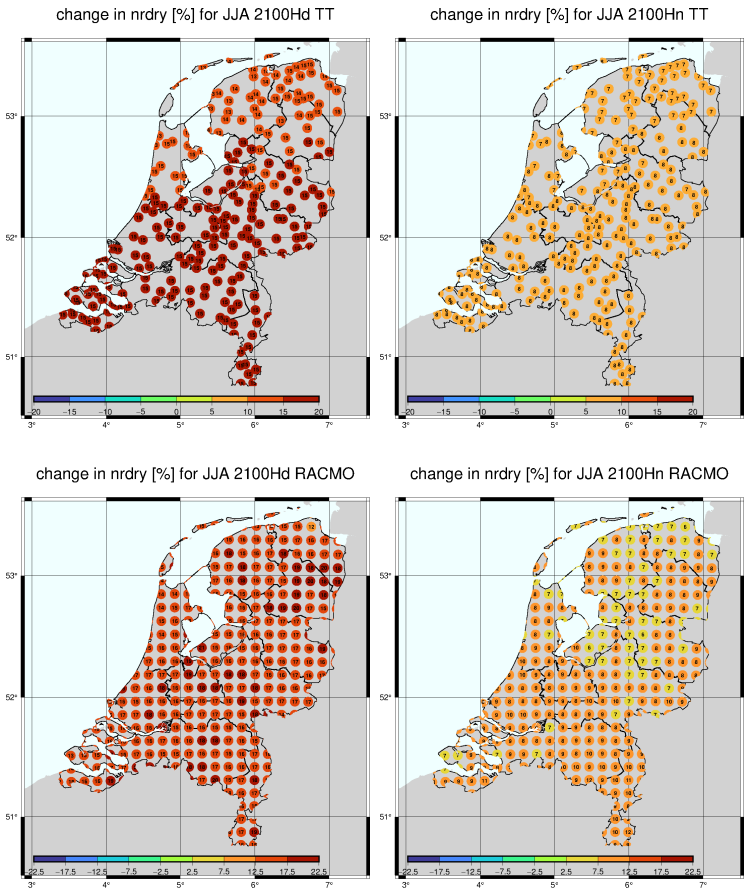

Fig. A19: Change in the number of dry days (threshold 1mm) in JJA for timeseries transformation (upper) and RACMO (lower) for the 2100Hd (left) and 2100Hn (right) scenario.

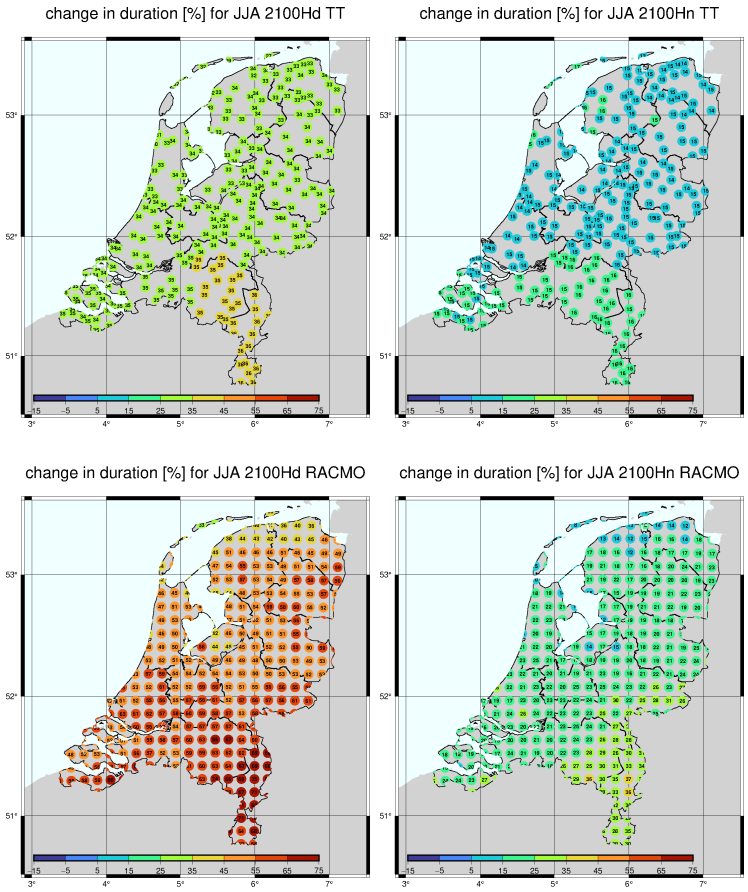

Fig. A20: Change in the duration of dry days (threshold 1mm) in JJA for timeseries transformation (upper) and RACMO (lower) for the 2100Hd (left) and 2100Hn (right) scenario.

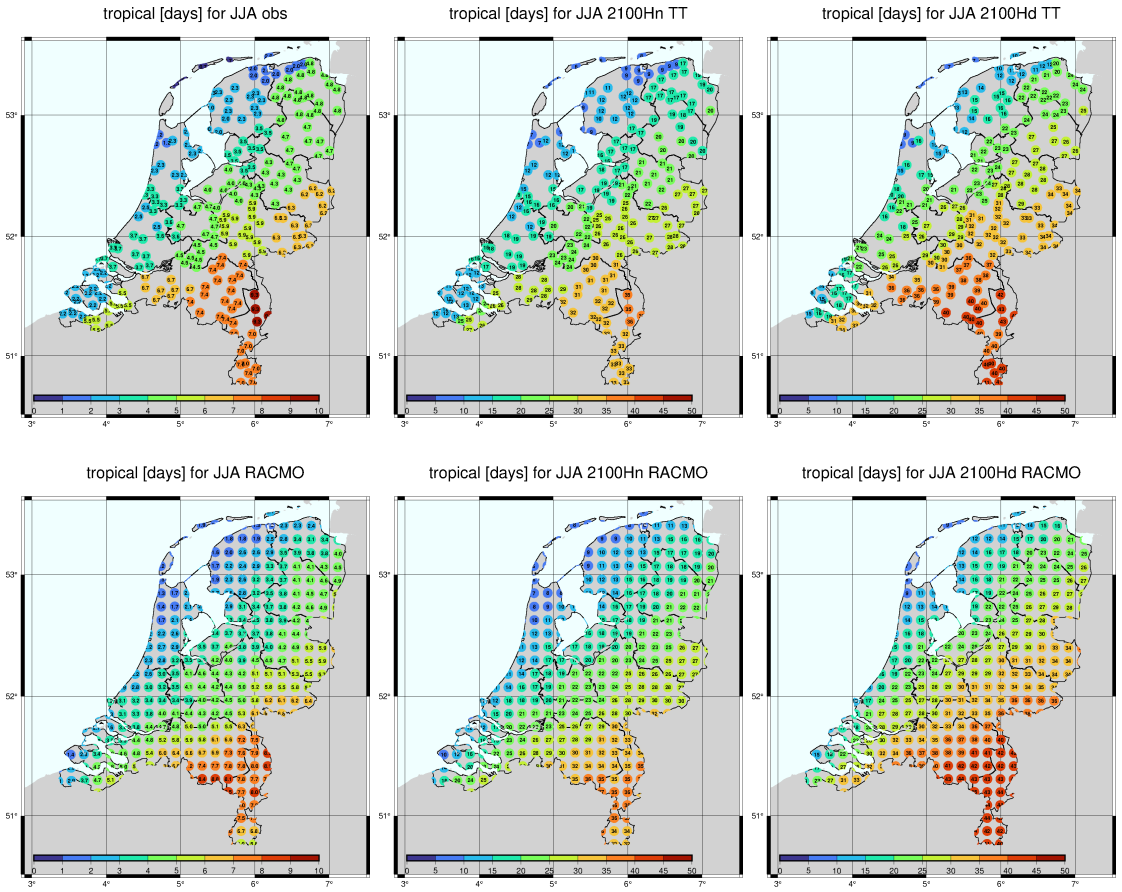

Fig. A21: Number of tropical days according to observations (left), TT for 2100Hn (middle) and 2100Hd (right), and for the BC RACMO runs (lower row).